ISBN: 978-3-95450-132-8 doi:10.18429/JACoW-IPAC2014-TUPME014

DEVELOPMENT OF SIX-DIMENSIONAL HELICAL MUON BEAM COOLING CHANNEL FOR MUON COLLIDERS *

K. Yonehara†, Fermilab, Batavia, IL 60510, USA

Abstract

The equilibrium transverse and longitudinal emittances in six-dimensional (6D) helical muon ionization cooling channel (HCC) has been investigated as functions of a solenoidal field strength and a helical field gradient with analytic method. As a result, the equilibrium emittance is determined by the solenoid field strength while the cooling partition and acceptance are strongly dependent on the helical field gradient. The HCC performance will be optimized by tuning these field components. The analysis shows the flexibility of HCC for multi-TeV and Higgs factory muon colliders.

INTRODUCTION

Fast 6D helical muon beam ionization cooling channel has been proposed [1]. Recent cooling simulation shows that the HCC achieves $\sim 10^6$ of 6D emittance reduction in 250 m [2]. The HCC consists of a helical dipole and solenoid magnetic components to generate a continuous dispersion in the Larmor motion. The helical field gradient is superimposed to stabilize the beam phase space and adjust the dispersion in the HCC. Hydrogen gas-filled RF cavities are incorporated continuously into the HCC magnet, in which muons lost their kinetic energy via the ionization process in dense hydrogen gas and simultaneously regain the lost energy from the RF field.

One of the challenges in the HCC design is incorporating a RF cavity into the HCC magnet. Several design efforts for the HCC beam element are in progress. A compact RF cavity has been considered by inserting a dielectric material [3,4]. Or a reentrant RF system has been proposed [5]. The recent RF design study shows that the RF cavity radius can be reduced by 25 % from a conventional pillbox RF cavity by using these techniques.

On the other hand, a large bore HCC magnet design has been studied and developed [6,7]. The most difficulties in the magnet design is generating a high helical field gradient with a large inner bore. Such a high gradient requirement is came from the original HCC design, which is based on the equal cooling decrements. Here, we break the cooling constraint and re-evaluated the cooling performance as functions of the solenoid field strength and helical field gradient.

Consequently, although the achievable equilibrium transverse and longitudinal emittances are changed by the helical field gradient the 6D equilibrium emittance is determined only by the solenoid field strength. On the other hand, the acceptance of the HCC is strongly dependent on the helical field gradient. The result suggests that the HCC field configuration must be modulated along with the channel length, i.e. the initial HCC must have a large acceptance and the final one must produce the lowest equilibrium 6D emittance in a strong solenoid magnet within the minimum engineering constraint.

HCC FORMULAE

Equilibrium emittance in the HCC is given from the analytic formulae [1]. Here, we show the formulae what we use in the document.

$$\varepsilon_s = \frac{\Lambda}{4\Lambda_\gamma}\frac{m_e}{m_\mu}\gamma\beta^2\left(\frac{\eta}{\omega Q_s}\frac{\gamma^2+1}{2\log}+\frac{(Z+1)fr_{ms}}{\gamma^2\beta^6}\frac{\omega Q_s}{\eta k^2}\frac{\hat{D}^2\kappa^2}{1+\kappa^2}\right) \quad (1)$$

$$\varepsilon_\pm = \frac{\Gamma_\pm}{4kQ_\pm}\frac{m_e}{m_\mu\beta}\frac{\Lambda/\Lambda_\pm}{(1+\kappa^2)^{5/2}}, \quad (2)$$

$$\Gamma_\pm = \frac{(Z+1)fr_{ms}(\alpha_\pm^2+(1+\kappa^2)^3Q_\pm^2)}{\alpha_\pm^2+(1+\kappa^2)\hat{D}^{-1}} + \frac{\kappa^2(\alpha_\pm-(1+\kappa^2)^{3/2})^2(\gamma^2+1)/2\log}{\alpha_\pm^2+(1+\kappa^2)\hat{D}^{-1}}, \quad (3)$$

where $fr_{ms} = \bar{X_0}/X_0$ is the correction factor to involve the Be window effect in the equilibrium emittance formulae. The cooling decrements are given,

$$\frac{\Lambda_+ + \Lambda_-}{\Lambda_0} = 2 - \frac{\kappa^2}{1+\kappa^2}\hat{D}, \quad (4)$$

$$\frac{\Lambda_+ - \Lambda_-}{\Lambda_0} = \frac{1}{\sqrt{R^2-G}}\left(q^2-1+\kappa^2\left(R\hat{D}-1\right)\right)\frac{1}{1+\kappa^2}, \quad (5)$$

$$\Lambda_+ + \Lambda_- + \Lambda_\gamma = 2\Lambda_0\left(\beta^2+\frac{1-(\beta/\gamma)^2}{\log}\right) \equiv \Lambda, \quad (6)$$

$$\Lambda_0 = \frac{F}{\gamma\beta^2 m_\mu}, \quad (7)$$

$$F = \frac{dE}{ds} = \frac{4\pi Zne^4\log}{m_e\beta^2}, \quad (8)$$

A drag force due to the ionization process F should also be corrected by the Be window thickness. Finally, we show the admittance of the HCC in the later discussion,

$$(I_s)_{adm} = \frac{2}{\pi\omega}\sqrt{\frac{\gamma'_{max}}{\eta\omega}}, \quad (9)$$

$$\eta = \frac{d}{d\gamma}\frac{\sqrt{1+\kappa^2}}{\beta} = \frac{\sqrt{1+\kappa^2}}{\gamma\beta^3}\left(\frac{\kappa^2}{1+\kappa^2}\hat{D}-\frac{1}{\gamma^2}\right), \quad (10)$$

where ω and γ' are the resonant RF frequency and the maximum energy deviation with respect to the path length, respectively. $\hat{D}$, log, k, κ, X_0, $\bar{X_0}$, Q_s, $Q_\pm$, $\alpha_\pm$, R, and G are given in refs. [1,8].

* Work supported by Fermilab Research Alliance, LLC under Contract No. DE-AC02-07CH11359 and DOE STTR grant DE-SC0007634
† yonehara@fnal.gov

ISBN: 978-3-95450-132-8 doi:10.18429/JACoW-IPAC2014-TUPME014

Magnetic field calculation

All primary HCC magnetic field parameters, i.e. a helical dipole (b), a helical field gradient (b') and a solenoid (B_z) components, are specified by the dispersion function, $\hat{D}$.

$$q \to q(\hat{D}) = \sqrt{\frac{1+\kappa^2-1/2\kappa^2\hat{D}}{1+1/2\kappa^2\hat{D}/(1+\kappa^2)}} \quad (11)$$

$$B_z = pk\frac{1+q(\hat{D})}{e\sqrt{1+\kappa^2}}, \quad (12)$$

$$b = \kappa B_z \frac{1-1/(1+q(\hat{D})}{1+\kappa^2}, \quad (13)$$

$$g = \hat{D}^{-1} - \frac{\kappa^2+(1-\kappa^2)q(\hat{D})}{1+\kappa^2}, \quad (14)$$

$$\frac{db_\phi}{dr} = b' = \frac{-egpk^2}{(1+\kappa^2)^{3/2}}, \quad (15)$$

where q is a reference to show the ratio between solenoid and helical dipole field strengths. Eq. (11) is derived from the condition in which the cooling decrements in the two eigen modes are equal, i.e. $\Lambda_+ = \Lambda_-$ in eq. (5).

Equal cooling decrements

In case of the equal cooling decrements, $\Lambda_\gamma = \Lambda_+ = \Lambda_- = \Lambda/3$, the dispersion factor can be defined from eq. (4),

$$\hat{D} = \frac{2(1+\kappa^2)}{\kappa^2}\left(1-\frac{2}{3}\left(\beta^2+\frac{1-(\beta/\gamma)^2}{\log}\right)\right). \quad (16)$$

The design momentum is 200 MeV/c, $\kappa = 1$, and the gas pressure is 160 atm at room temperature, the dispersion function is ~1.92. The HCC field components can be calculated from eqs. (11) ~ (15) at the helical period 0.5 m, these are $B_z = 10.9\ T$, $b = 2.49\ T$, and $b' = -0.825\ T/m$. It is challenging to generate such a strong focusing, b' with keeping an enough space to incorporate the RF cavity into the magnet in the present HCC magnet design [6, 7].

EQUILIBRIUM EMITTANCE AS FUNCTIONS OF B_z AND b'

The equilibrium transverse and longitudinal emittances can be tuned by the helical field gradient, i.e. the dispersion factor. Figures 1 and 2 show the equilibrium transverse and longitudinal emittances as a function of B_z where the dispersion factor is changed from 0.92 to 2.2 with various helical periods (λ). The beam stability condition which is given in refs. [1] and [8] is satisfied with the dispersion factor. Shorter helical period, thus stronger solenoid field makes lower transverse and longitudinal emittances. However, lower equilibrium (higher) transverse emittance makes higher (lower) equilibrium longitudinal emittance.

This correlation becomes more obvious in the helical field gradient dependence, b' plots shown in figures 3 ~ 4. Stronger helical field gradient makes lower transverse equilibrium and higher longitudinal equilibrium emittances.

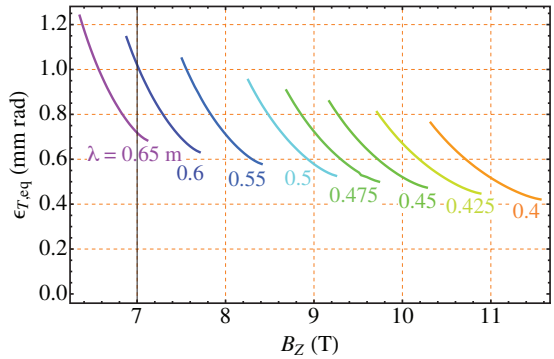

Figure 1: Calculated transverse equilibrium emittance.

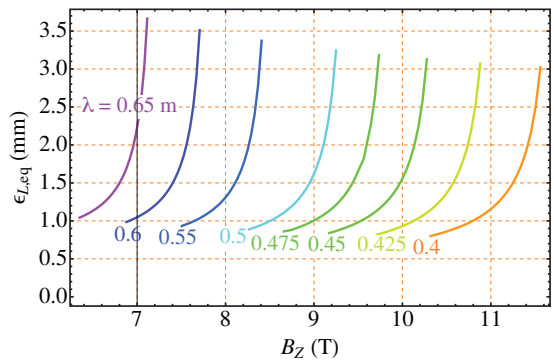

Figure 2: Calculated longitudinal equilibrium emittance.

On the other hand, the available helical field gradient in the present HCC magnet design is up to -2~3 T/m at helical period 0.4 m. Therefore, the achievable equilibrium transverse emittance is ~0.65 $mmrad$. It should be noted that the overall 6D emittance, i.e. $\varepsilon_{6D} \sim \varepsilon_{T,eq}^2\varepsilon_{L,eq}$ is constant in a fixed helical period.

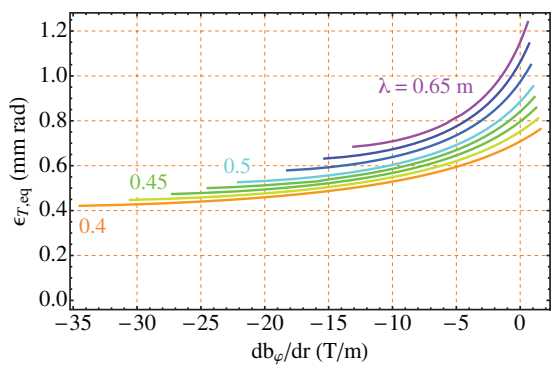

Figure 3: Estimated transverse equilibrium emittance.

Similar investigation has been made with various helical pitches, κ. Figures 5 ~ 6 show the equilibrium transverse and longitudinal emittances with various κ, respectively. The achievable 6D emittance becomes smaller in larger κ. It is because stronger B_z is generated in larger κ.

ISBN: 978-3-95450-132-8 doi:10.18429/JACoW-IPAC2014-TUPME014

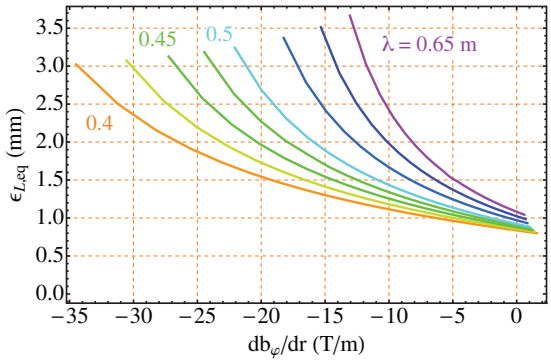

Figure 4: Estimated longitudinal equilibrium emittance.

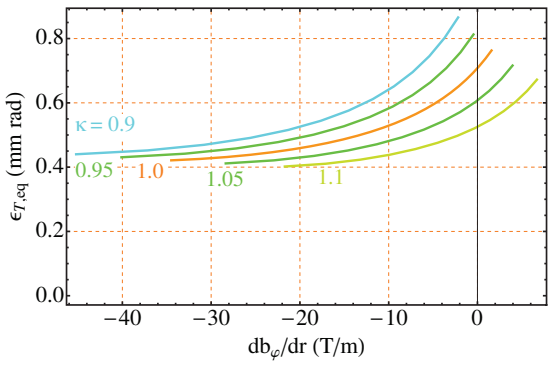

Figure 5: Estimated transverse equilibrium emittance.

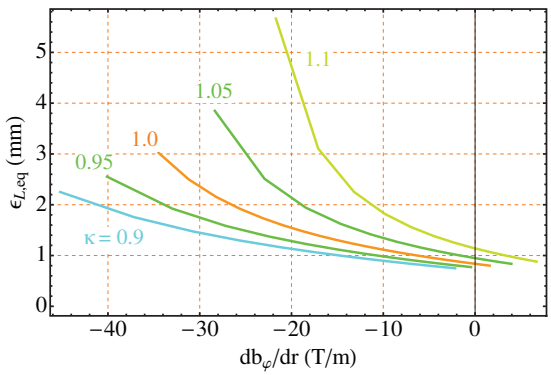

Figure 6: Estimated longitudinal equilibrium emittance.

MOMENTUM ACCEPTANCE

The momentum acceptance is given by the admittance of the HCC in eqs. (9) and (10). The admittance is dependent on the dispersion factor. Figure 7 shows the observed momentum acceptance of the HCC in G4BL [9] (red point) and the prediction from eqs. (9) and (10) (red dashed line). The prediction agrees very well with the numerical result. Lower dispersion factor makes larger momentum acceptance.

NEW EMITTANCE EVOLUTION

The initial HCC must have a low dispersion to increase the momentum acceptance. Once the momentum spread is adequate to the final HCC section the solenoid field should be maximized to obtain the lowest 6D emittance. Here is the exercise. The HCC magnet with the solenoid field 11 T and the helical field gradient 0 T/m in the helical period 0.36 m, the achievable transverse and longitudinal emittances is 0.6 $mmrad$ and 0.5 mm, respectively. Reverse emittance exchange takes place in a match-out section where the helical beam orbit is untangled into the straight beam in a straight solenoid low field channel [10]. Thus, the longitudinal emittance grows, e.g. $0.5 \rightarrow 1.5$ mm the transverse emittance is reduced $0.6 \rightarrow 0.6/\sqrt{3} = 0.35$ $mmrad$. These emittances are close to the goal for multi-TeV muon colliders. Or, the HCC can generate very small energy spread muon beam which is useful for a Higgs factory muon collider. The numerical investigation is underway.

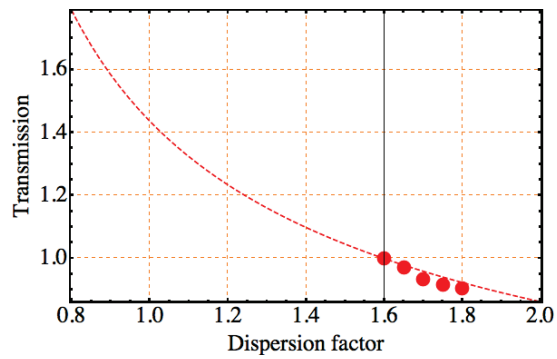

Figure 7: Momentum acceptance as a function of dispersion factor. Lower dispersion makes larger acceptance.

REFERENCES

[1] S. Derbenev, R.P. Johnson, Phys. Rev. ST Accel. Beams 8, 041002 (2005).

[2] C. Yoshikawa et al., "Complete Muon Cooling Channel Design and Simulations", IPAC'13, China, June 2013, TUPFI060 (2013).

[3] K.D. French, Nucl. Instrum. Meth., A624, 731 (2010).

[4] L. Nash et al., "High Power Tests of Alumina in High Pressure RF Cavities for Muon Ionization Cooling Channel", IPAC'13, China, June 2013, TUPFI068 (2013).

[5] F. Marhauser et al., "RF Cavity Design Aspects for a Helical Muon Beam Cooling Channel", IPAC'14, Dresden, Germany, June 2014, THPME054, These Proceedings.

[6] M.L. Lopes et al., "Magnetic Design Constraints of Helical Solenoids", IPAC'14, Dresden, Germany, June 2014, WEPRI100, These Proceedings.

[7] S.A. Kahn et al., "Elliptical Muon Helical Cooling Channel Coils to Incorporate RF Cavities", IPAC'14, Dresden, Germany, June 2014,TUPRO116, These Proceedings.

[8] K. Yonehara, "Study Cooling Performance in a Helical Cooling Channel for Muon Colliders", IPAC'14, Dresden, Germany, June 2014, TUPME015, These Proceedings.

[9] T.J. Roberts, http://www.muonsinternal.com/muons3/G4beamline

[10] C. Yoshikawa, "Status of the Complete Muon Cooling Channel Design and Simulation", IPAC'14, Dresden, Germany, June 2014, TUPME016, These Proceedings.